A Novel Four-Port UWB MIMO Metasurface Antenna for mmWave Applications

Ruwaybih Alsulami
Department of Electrical Engineering, Umm Al-Qura University, Makkah, Saudi Arabia
rrsulami@uqu.edu.sa (corresponding author)

Sulaiman Alharbi
Department of Electrical Engineering, Umm Al-Qura University, Makkah, Saudi Arabia
s441003645@uqu.edu.sa

Abdulelah Alotaibi
Department of Electrical Engineering, Umm Al-Qura University, Makkah, Saudi Arabia
s441005962@uqu.edu.sa

Saad Alqurashi
Department of Electrical Engineering, Umm Al-Qura University, Makkah, Saudi Arabia
s441002258@uqu.edu.sa

Aseel Alrddadi
Department of Electrical Engineering, Umm Al-Qura University, Makkah, Saudi Arabia
s441007997@uqu.edu.sa

Abdurahman Alharbi
Department of Electrical Engineering, Umm Al-Qura University, Makkah, Saudi Arabia
s441000748@uqu.edu.sa

Saeed Alzahrani
Department of Electrical Engineering, University of Tabuk, Tabuk, Saudi Arabia
saeedalzahrani@ut.edu.sa

Received: 12 August 2025 | Revised: 18 September 2025 and 7 October 2025 | Accepted: 12 October 2025

 DOI: https://doi.org/10.48084/etasr.14036

ABSTRACT

This paper introduces a new Ultra-Wideband (UWB) metasurface-based Millimeter-Wave (mmWave) Multiple-Input Multiple-Output (MIMO) antenna designed for mmWave applications. The proposed MIMO antenna, incorporating a metasurface, achieves a wide fractional bandwidth of 66.1%, covering frequencies from 23.33 GHz to 46.4 GHz. It delivers a peak gain of 11 dB with a variation of 3.5 dB across the band and maintains high radiation efficiency between 91.7% and 95.2%. With a minimal footprint of 32 × 32 mm², the design integrates four antenna arrays. First, a single antenna array is optimized for UWB performance and enhanced gain using a metasurface. Next, a MIMO configuration is developed, preserving the performance of the single antenna while incorporating a metasurface for further gain improvement. The antenna supports multiple mmWave bands, including the 24 GHz Industrial, Scientific, and Medical (ISM) band, the K-band, the Ka-band (27–40 GHz), and key mmWave frequencies such as 26 GHz, 28 GHz, and 38 GHz. This design demonstrates strong potential for high-performance mmWave communication systems.

Keywords-Multiple-Input Multiple-Output (MIMO) antenna; Ultra-Wideband (UWB); metasurface antenna; Millimeter-Wave (mmWave); UWB MIMO

I. INTRODUCTION

In recent years, the demand for higher data transmission rates has continued to grow, leading to increased pressure on existing frequency bands and a shortage of available spectrum. To address this challenge, communication systems are shifting toward Millimeter-Wave (mmWave) frequencies, which offer wider bandwidth and less signal interference due to their shorter wavelengths, making Ultra-Wideband (UWB) mmWave technology a promising solution for achieving faster data rates and overcoming spectrum limitations [1-7]. Recent works have designed UWB antennas for mmWave use cases to increase data rates; moreover, UWB antennas support many mmWave bands for different applications and offer advantages such as low latency, high resolution, and high precision [1-6].

In modern communication systems, multiple antennas are expected to be used at both user devices and base stations, making Multiple-Input Multiple-Output (MIMO) technology and antenna arrays essential components; antennas, as core elements, are key to developing wireless devices that are efficient, cost-effective, and compact, and, as a result, significant research has focused on designing broadband, high-gain, and compact MIMO antennas to meet the needs of modern wireless communication systems. To improve channel capacity through greater bandwidth or transmit power, MIMO configurations are incorporated into designs; MIMO and massive-MIMO (m-MIMO) employ multiple components at both the transmitting and receiving ends, enhancing spectral efficiency, data rates, and capacity [6-12]. Combining wider bandwidth with MIMO can further amplify these benefits, motivating research on UWB MIMO antennas to explore their potential [6, 7, 9, 10, 12].

To enhance the performance of the antenna, particularly its power gain, a metasurface is employed while ensuring the compactness of the design [13-16]. A metasurface is an artificially constructed structure composed of regularly arranged Perfect Electric Conductors (PECs) on a dielectric substrate, backed by a metallic layer, which does not exist naturally. The metasurface exhibits a remarkable ability to manipulate and control the properties and behavior of Electromagnetic (EM) waves that interact with it. By applying modifications to the EM waves, the metasurface introduces improvements in terms of antenna gain, leading to enhanced performance [15]. Therefore, the metasurface technique is used for the UWB MIMO antenna to further improve its power gain. Researchers have studied UWB MIMO antennas with metasurfaces to improve the power gain. In [17], authors presented a 4-element UWB MIMO antenna with a metasurface that operates at the 24.55–26.5 GHz frequency range. A metasurface array of 9 × 6 Circular Split Ring (CSR) resonators was employed, achieving a peak gain of 10.27 dBi and improving isolation by 5 dB, with a minimum isolation of −38 dB. The study in [18] proposed a 2 × 2 metasurface placed underneath a four-element antenna array that operated from 23.3 GHz to 28.8 GHz with more than 80% efficiency and achieved a peak gain of 10.44 dBi. In [19], authors presented a compact 4-port UWB MIMO antenna utilizing orthogonal element orientation and Defective Ground Structure (DGS), achieving an operational bandwidth of 25–50 GHz with high isolation (>20 dB). The study in [20] showed a quad-port MIMO antenna with an X-shaped decoupling structure, achieving a wideband operation from 22.5 GHz to 29.2 GHz and a peak gain of 4.25 dBi. In [21], authors presented a quad-port MIMO antenna with a Frequency-Selective Surface (FSS) array and DGS techniques, achieving a UWB operation from 23.57 GHz to 39.35 GHz, a peak gain of 7.78 dBi, and high isolation (>31 dB).

In this study, a novel UWB MIMO antenna array with enhanced gain, employing a metasurface, is presented as a promising solution for a wide range of mmWave applications. The antenna size is 32 × 32 mm^2, and it has been specifically designed on a Roger RT−5880 substrate that enables high-frequency operation. The utilization of this substrate material ensures optimal performance and compatibility with the desired frequency range. With its improved gain characteristics and compact size, this novel UWB antenna array holds great potential for diverse mmWave applications.

II. PROPOSED UWB MIMO ANTENNA WITH METASURFACE

Several design techniques are applied to the proposed antenna to achieve UWB performance with enhanced gain, making it suitable for mmWave applications. As shown in Figure 1, the proposed UWB metasurface MIMO antenna consists of two separate metal layers. The first substrate includes the MIMO antenna arrays and a ground plane, whereas the second is a single metal layer dedicated to the metasurface. Both substrates are fabricated using RT-5880, a material selected for its excellent high-frequency properties. The following sections describe the single UWB antenna array, both without and with the metasurface, including its dimensions and simulation results. Subsequently, the design and performance of the MIMO antenna with the integrated metasurface are discussed.

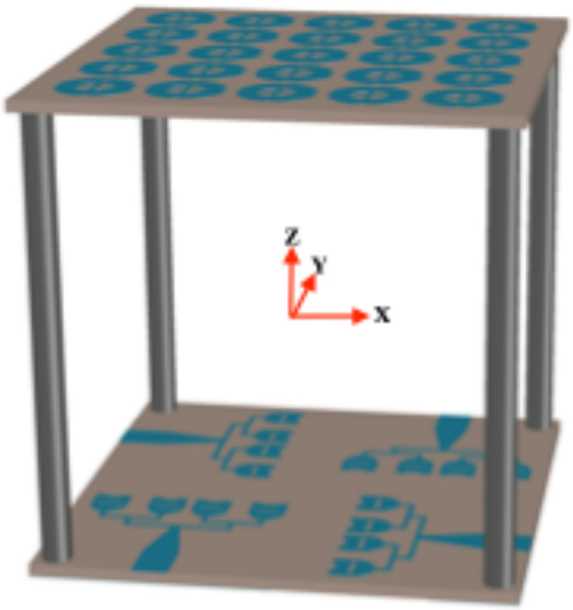

Fig. 1. Proposed novel UWB MIMO metasurface antenna.

A. Single Antenna Design and Performance Analysis

1) Antenna Array without Metasurface Design

The single antenna array design incorporates a two-layer metallic substrate, as shown in Figure 2. Figure 2(a) provides a visualization of the top metal layer, whereas Figure 2(b) illustrates the bottom layer functioning as the ground plane. To enhance the antenna's gain while maintaining a compact size, a 4 × 1 antenna array configuration is employed in the proposed design. Furthermore, a rectangular slot is strategically positioned in the center of the radiating patch for each element, effectively altering the current distribution to achieve a broader frequency response. Additionally, a semi-oval slot is introduced at the top of the radiating patch for each element to enhance the bandwidth. In terms of the feedline, it is designed to have a 50 Ω impedance to ensure compatibility with the SMA connector. Furthermore, the feedline width gradually decreases as it moves away from the port, resulting in an increase in characteristic impedance. This intentional adjustment leads to improved antenna performance in terms of gain and bandwidth.

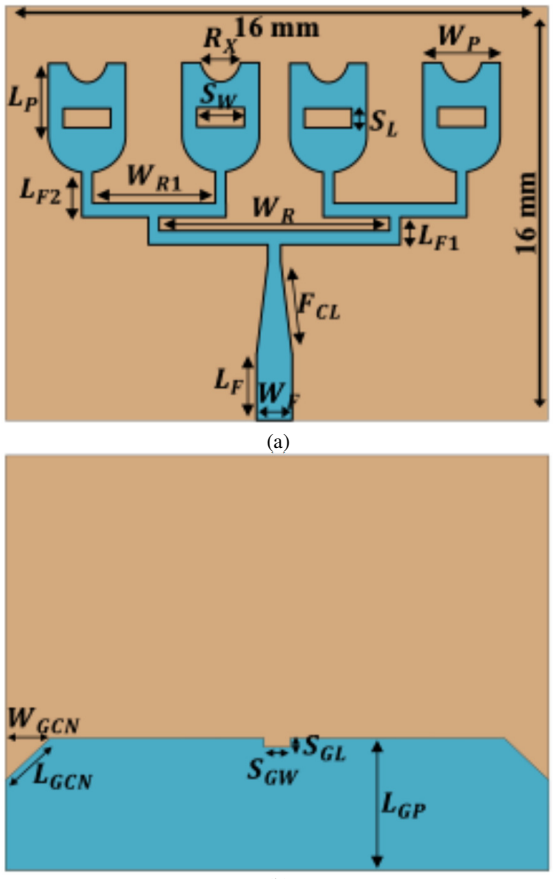

Fig. 2. Single UWB antenna array substrate: (a) top layer, (b) bottom layer.

In Figure 2(b), the DGS technique is employed to assist in achieving UWB performance, as described in [22]. Furthermore, middle and corner slots are implemented to effectively mitigate the reflection coefficient. The specific dimensions of the two-layer metal antenna array substrate can be found in Table I.

TABLE I. SINGLE UWB ANTENNA ARRAY DIMENSIONS

Top layer					
W_P	L_P	R_X	S_W	S_L	L_{F2}
2.5	1.6	0.6	1.5	0.5	1.0
W_{R1}	L_{F1}	W_R	F_{CL}	L_F	W_F
4.1	0.6	7.4	4.09	3.0	2.42
Bottom layer					
L_{GP}	S_{GL}	S_{GW}	W_{GCN}	L_{GCN}	
7.3	0.5	0.7	1.5	2.12	

a. All units are in mm.

The reflection coefficient (S_{11}) simulation result without the metasurface is shown in Figure 3. The antenna operating frequencies are from 23.12 GHz to 45.92 GHz, providing an absolute bandwidth of 22.8 GHz. The fractional bandwidth of the proposed antenna is 66.05%. In Figure 4, the power gain and radiation efficiency without the metasurface are shown. The power gain for the proposed antenna varies from 5.54 dB to 8.0 dB across the operating frequencies, whereas the radiation efficiency ranges from 83.9% to 94.8%.

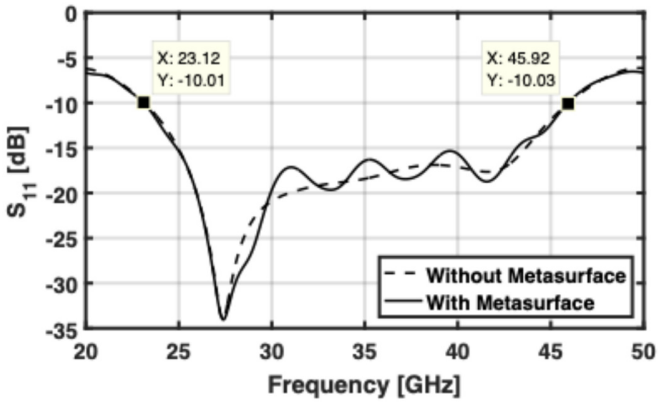

Fig. 3. Simulation results of the reflection coefficient (S_{11}) for the single UWB antenna array with and without the metasurface.

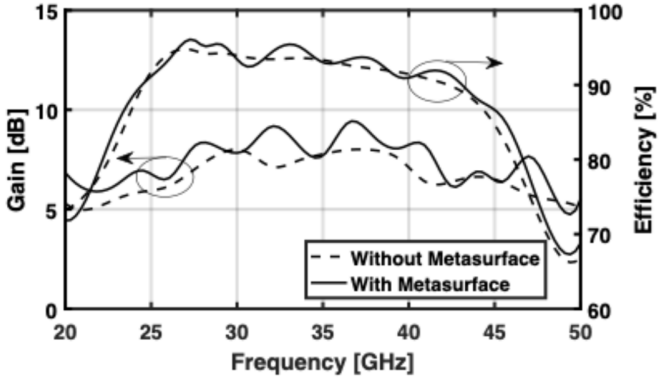

Fig. 4. Simulation results of the power gain and radiation efficiency for the single UWB antenna array with and without the metasurface.

2) Antenna Array Metasurface Design

The proposed structure of the metasurface unit cell, including its dimensions, is shown in Figure 5. The metasurface is a type of metamaterial consisting of a unit cell, which is repeated periodically in a two-dimensional form [23]. The proposed metasurface is an absorption metasurface, designed to effectively absorb electromagnetic waves at specific frequencies [24]. This particular type of metasurface is constructed using a single metal layer on an RT-5880 substrate without the presence of a ground plane.

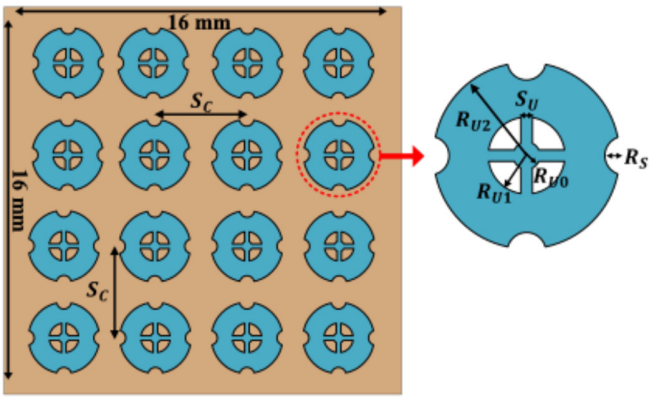

Fig. 5. Single UWB antenna array with a 4 × 4 metasurface structure.

The proposed metasurface unit is designed to operate across the target UWB frequency range. The structure includes four slots at the center and four rounded notches along the edges. These features introduce multiple resonances, which together create the UWB response. The slots and notches function by modifying the current paths and adding capacitive coupling, generating the resonant modes. Several design iterations were performed to refine the geometry and achieve the final unit structure. The dimensions of the proposed unit cell for the metasurface can be found in Table II. Furthermore, a 4 × 4 arrangement of periodic cells is employed for the metasurface. The vertical and horizontal gaps between these metasurface cells are identical. To attach the metasurface above the antenna array, vias with a spacing of 3 mm are utilized, and nylon material with a dielectric constant of 3.7 is employed for the vias. The impact of mounting the metasurface at various angles was investigated, but it was found to have a negligible effect.

TABLE II. SINGLE ANTENNA ARRAY METASURFACE DIMENSIONS

Single (top) layer					
R_{U0}	R_{U1}	R_{U2}	R_S	S_U	S_C
0.15	0.72	1.54	0.30	0.14	4.0

a. All units are in mm.

3) Simulation Results of the Single Antenna Array with Metasurface

After integrating the metasurface on top of the antenna array using vias, the proposed antenna was simulated using EM software. The S_{11} magnitude result, shown in Figure 3, is similar to that of the antenna array without the metasurface, with a fraction bandwidth of 66.05%. However, improvements are observed in gain and efficiency, as shown in Figure 4. The power gain varies from 6.12 dB to 9.4 dB across the operating frequencies, with a maximum gain increase of 1.4 dB compared to the antenna without the metasurface. The radiation efficiency varies from 86.2% to 96.1%, with an increase of 1.3% at the peaks. These findings highlight the advantages of using a metasurface with the UWB antenna. The radiation patterns of the proposed novel metasurface antenna were simulated at multiple frequencies: 28 GHz, 32 GHz, and 38 GHz.

The simulated radiation patterns are shown in Figure 6, with the elevation plane (E-plane) and azimuth plane (H-plane) depicted in Figures 6(a) and 6(b), respectively. The E-plane provides information about the antenna's radiation characteristics in the vertical direction, and shows that the antenna radiates in an omnidirectional pattern. The H-plane provides information about the antenna's radiation characteristics in the horizontal direction, and shows that the antenna radiates in a directional pattern.

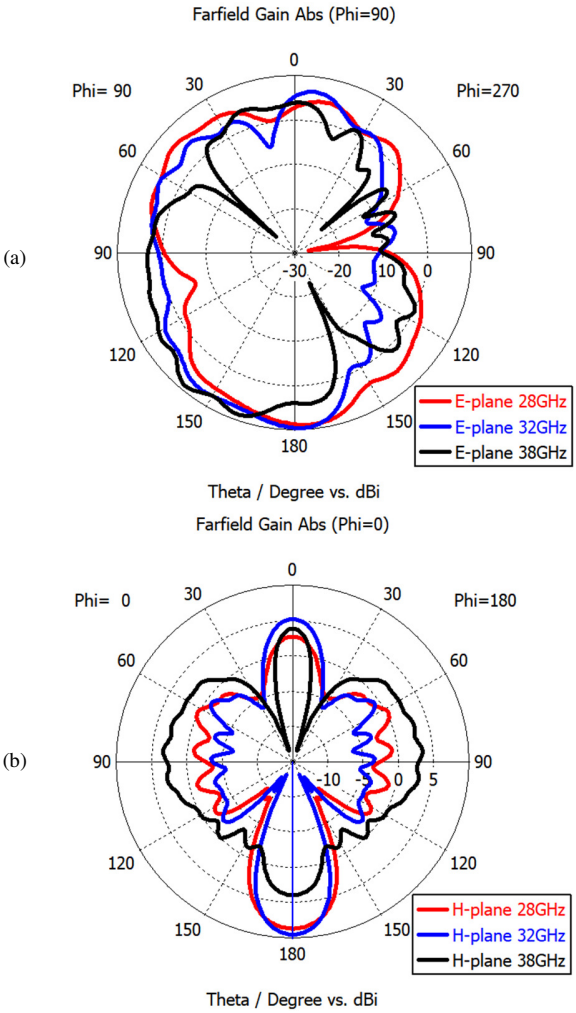

Fig. 6. Radiation patterns of the single antenna array with metasurface at different frequencies: (a) elevation plane (E-plane), (b) azimuth plane (H-plane).

B. Proposed MIMO Antenna Array with Metasurface

1) MIMO Antenna Implementation

In designing the proposed MIMO antenna array, several important factors are considered to ensure optimal performance. Maintaining the UWB characteristics observed in the single antenna array is a primary objective, along with further enhancing the gain. Additionally, the overall size of the MIMO antenna array is carefully addressed to achieve a compact design suitable for practical applications.

The configuration of the MIMO antenna's top and bottom layers are shown in Figures 7(a) and 7(b), respectively. In Figure 7(a), four single antenna arrays are arranged in an orientation that preserves UWB performance while minimizing the overall footprint, representing the optimal layout for this design. Each single antenna within the MIMO array retains the same dimensions for the top and bottom metal layers as previously specified. The spacing between the antenna elements, labeled as S_{P1}, S_{P2}, S_{P3}, and S_{P4}, is kept constant at 4.7 mm to maintain consistent performance across the array.

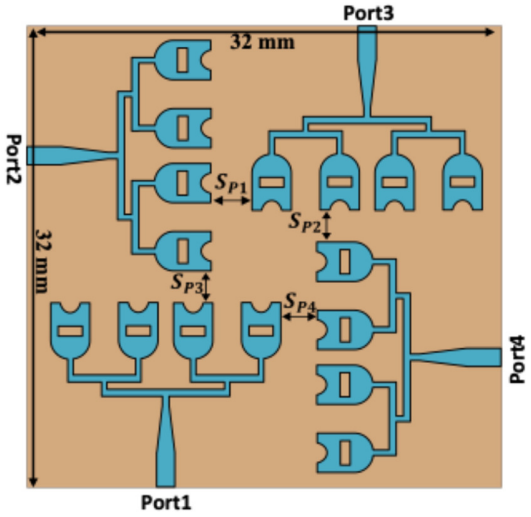

(a)

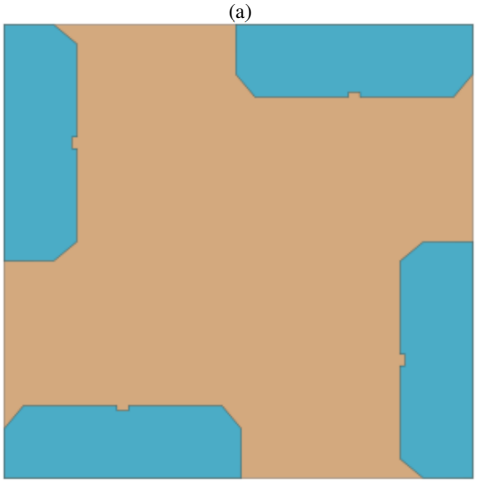

(b)

Fig. 7. Structure of the proposed UWB MIMO antenna array: (a) top layer, (b) bottom layer.

2) MIMO Antenna Metasurface Construction

The proposed MIMO antenna's metasurface configuration is illustrated in Figure 8. The metasurface unit cell structure is the same as that used for the single antenna array, but the number of metasurface cells and dimensions are different. To accommodate the increased size in the MIMO configuration, the metasurface cell size is increased, and the number of cells in the metasurface layer is set to 5 × 5. All relevant dimension values are provided in Table III. This approach ensures that the MIMO antenna array remains compact, retains its UWB properties, and benefits from the performance enhancements offered by the optimized metasurface design.

TABLE III. MIMO ANTENNA ARRAY METASURFACE DIMENSIONS

Single (top) layer					
R_{U0}	R_{U1}	R_{U2}	R_S	S_U	S_C
0.25	1.30	2.60	0.30	0.28	5.8

a. All units are in mm.

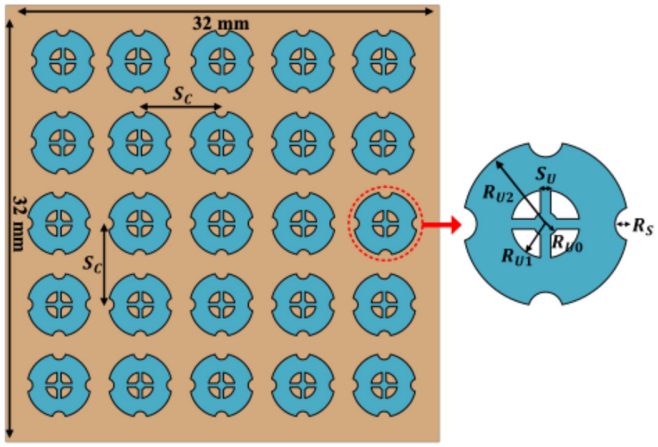

Fig. 8. UWB MIMO antenna with a 5 × 5 metasurface structure.

3) Simulation Results of the Proposed MIMO Antenna Array

The reflection coefficients (S_{11}) of the proposed MIMO antenna array, both with and without the metasurface, are shown for ports 1 and 4 in Figure 9(a). Ports 1 and 4 are selected for illustration, as the other ports exhibit nearly identical behavior. The results demonstrate that the reflection coefficients for all four ports remain very similar regardless of the presence of the metasurface. The proposed MIMO antenna with metasurface has an absolute bandwidth of 23.07 GHz and a fractional bandwidth of 66.1%. In addition, Figure 9(b) displays the isolation coefficients between all four ports. These values consistently remain below -20 dB, indicating strong isolation and effective suppression of mutual coupling within the MIMO antenna array.

Figure 10 presents the measured power gain and radiation efficiency for the MIMO antenna array in both configurations: with and without the metasurface. A clear improvement in gain is observed when the metasurface is integrated into the design, highlighting its positive impact on antenna performance. Specifically, the MIMO antenna with metasurface achieves a peak gain of 11.0 dB at 30.5 GHz, with the gain fluctuating by

3.5 dB across the entire operating frequency band. This indicates that the metasurface not only enhances the peak gain but also contributes to maintaining stable gain performance throughout the bandwidth. In terms of radiation efficiency, both configurations demonstrate consistently high values, ranging from 91.7% to 95.2% across the operating frequencies. The addition of the metasurface does not introduce significant losses, as the efficiency curves for both cases remain closely aligned. These results confirm that the metasurface effectively improves gain without compromising radiation efficiency.

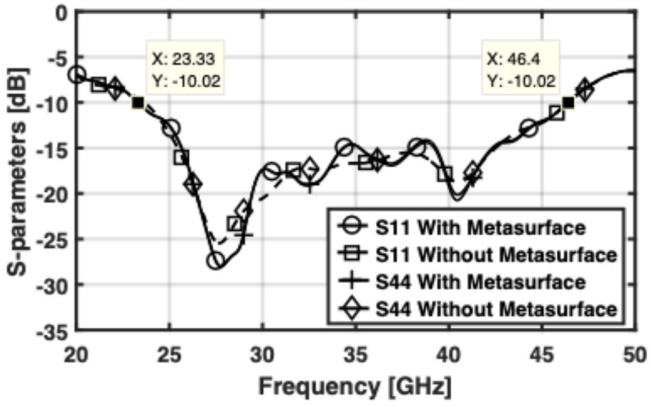

(a)

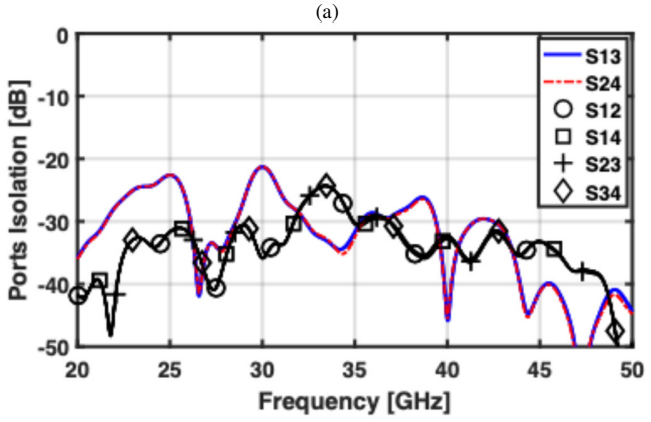

(b)

Fig. 9. S-parameters of the MIMO antenna array: (a) reflection coefficients with and without metasurface at ports 1 and 4, (b) isolation coefficients with metasurface between all four ports.

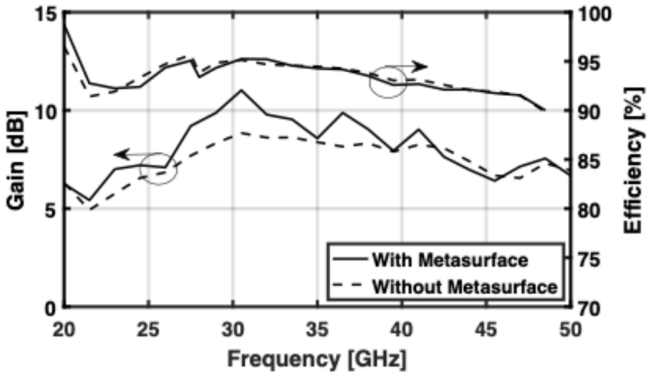

Fig. 10. Simulation results of the power gain and radiation efficiency for the MIMO antenna array with and without the metasurface.

Figure 11 shows the radiation patterns of the proposed UWB MIMO antenna at all four ports. In Figure 11(a), the elevation plane (E-plane) patterns are presented for each port, revealing consistent behavior despite the different antenna orientations. The E-plane patterns are bidirectional with multiple lobes, with the strongest radiation directed toward the broadside. Figure 11(b) shows the azimuth plane (H-plane) patterns for all four ports, which also demonstrate similar characteristics. The H-plane patterns are generally symmetrical, with broad main lobes and multiple side lobes. This uniformity in both E-plane and H-plane patterns across all ports highlights the antenna's ability to maintain stable and wide coverage, supporting effective MIMO performance and reliable signal transmission.

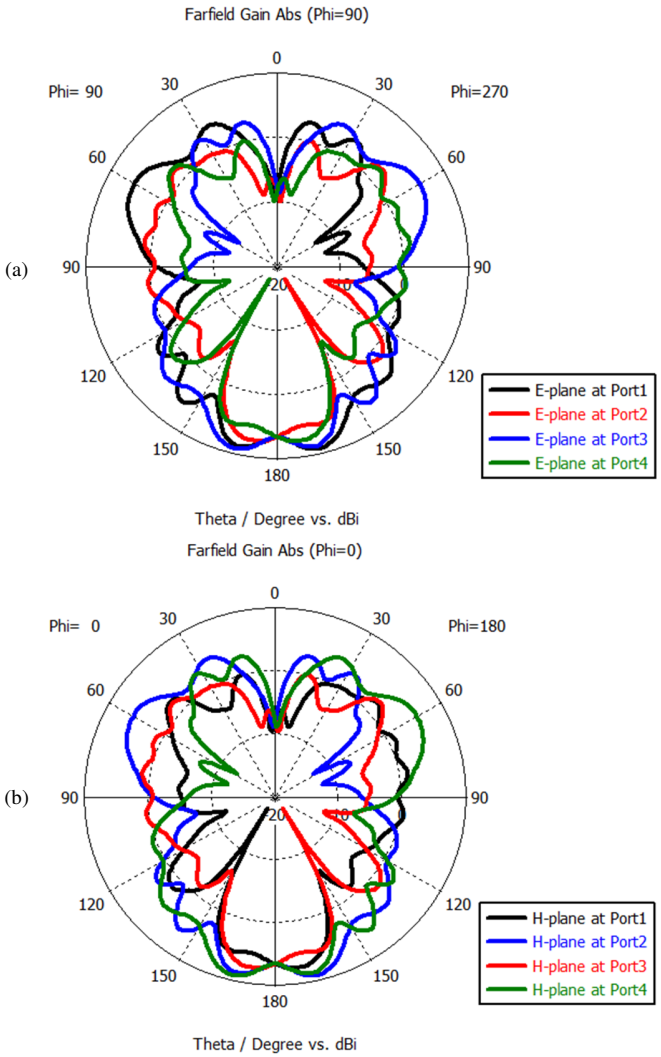

(a)

(b)

Fig. 11. Radiation patterns of the MIMO antenna array with metasurface at all four ports: (a) elevation plane (E-plane), (b) azimuth plane (H-plane).

C. Comparison with State-of-the-Art Works

A comparison of the proposed UWB MIMO antenna array with metasurface and other recently published similar works is presented in Table IV. It is observed the proposed MIMO

antenna with metasurface surpasses other reported works in terms of bandwidth and gain. Although the work reported in [22] achieves a higher bandwidth, the gain values reported (about 10 dB) correspond only to the diversity gain, meaning that the realized power gain will be significantly lower. In contrast, the proposed antenna achieves strong performance across multiple metrics, including wide bandwidth and high realized gain, leading to improved MIMO capabilities. These characteristics make the design highly suitable for both current and future wireless communication systems, where enhanced bandwidth and gain are essential.

TABLE IV. COMPARISON WITH RELATED WORK

Ref., year	Size (mm^2) /material	Freq. (GHz)	BW (%)	Peak gain (dBi)	Isolation (dB)	Port
[17], 2021	22 × 24 / RT-5880	23.5–29.4	22.3	10.44	< −20	4
[18], 2021	30 × 43 / RT-5880	24.5–26.4	7.26	10.27	< −45	4
[19], 2023	33 × 33 / RT-4003C	25–50	66.7	NA	< −10	4
[20], 2024	40 × 40 / RT-5880	22.5–29.2	25.9	4.25	< −27	4
[21], 2025	22 × 22 / RT-5880	23.6–39.3	50.1	7.78	< −31.52	4
This work	32 × 32 / RT-5880	23.3–46.4	66.1	11.0	< −20	4

III. CONCLUSION

This work presents a novel Ultra-Wideband (UWB) Multiple-Input Multiple-Output (MIMO) antenna array with an integrated metasurface, designed for millimeter-wave (mmWave) applications, achieving significant improvements in gain, bandwidth, and efficiency while maintaining stable radiation patterns across all ports. The design achieves an absolute bandwidth of 23.07 GHz and a high fractional bandwidth of 66.1%, supporting wideband operation. A peak gain of 11.0 dB is observed, whereas the radiation efficiency remains between 91.7% and 95.2% throughout the operating range. The isolation coefficients confirm strong port isolation and minimal mutual coupling, and the elevation plane (E-plane) and azimuth plane (H-plane) radiation patterns remain consistent across all ports, ensuring uniform coverage and robust spatial diversity. These results highlight the effectiveness of the metasurface in improving antenna performance without compromising efficiency, making this design a strong candidate for high capacity, wideband wireless

REFERENCES

[1] S. X. Ta, H. Choo, and I. Park, "Broadband Printed-Dipole Antenna and Its Arrays for 5G Applications," *IEEE Antennas and Wireless Propagation Letters*, vol. 16, pp. 2183–2186, 2017, https://doi.org/10.1109/LAWP.2017.2703850.

[2] S. Alzahrani and R. Alsulami, "38 GHz Wideband and High Gain Stacked Antenna Modelling for 5G Applications," in *2023 International Conference on Radar, Antenna, Microwave, Electronics, and Telecommunications*, Bandung, Indonesia, 2023, pp. 57–60, https://doi.org/10.1109/ICRAMET60171.2023.10366678.

[3] M. Awais, A. Riaz, and W. T. Khan, "An Ultra-wideband (16 40 GHz) mmWave Antenna for Automotive Radar and 5G Applications," in *2019 IEEE International Symposium on Antennas and Propagation and USNC-URSI Radio Science Meeting*, Atlanta, GA, USA, 2019, pp. 1919–1920, https://doi.org/10.1109/APUSNCURSINRSM.2019.8889255.

[4] P. Zhong, T. Wang, and S. Wang, "A UWB antenna for 5G millimeter wave frequency band," in *2020 International Conference on Microwave and Millimeter Wave Technology*, Shanghai, China, 2020, pp. 1–3, https://doi.org/10.1109/ICMMT49418.2020.9386829.

[5] A. Jabbar, J. ur R. Kazim, M. A. Imran, Q. H. Abbasi, and M. U. Rehman, "Design Of A Compact Ultra-Wideband Microstrip Antenna for Millimeter-Wave Communication," in *2021 IEEE International Symposium on Antennas and Propagation and USNC-URSI Radio Science Meeting*, Singapore, 2021, pp. 837–838, https://doi.org/10.1109/APS/URSI47566.2021.9704395.

[6] S. Sarade and S. D. Ruikar, "Development of a Wide Bandwidth Massive Eight Dissimilar Radiating Element Multiband MIMO Antenna for mm-Wave Application," *Engineering, Technology & Applied Science Research*, vol. 12, no. 5, pp. 9166–9171, Oct. 2022, https://doi.org/10.48084/etasr.5133.

[7] S. Sarade and S. D. Ruikar, "Development of Two UWB Multiband MIMO Antennas with Enhanced Isolation and Cross-Correlation," *Engineering, Technology & Applied Science Research*, vol. 13, no. 1, pp. 9166–9171, Feb. 2023, https://doi.org/10.48084/etasr.5422.

[8] P. Ramya *et al.*, "Enhancing 5G Performance: A Study of an MIMO Antenna with Elliptical Ring Polarization," *Engineering, Technology & Applied Science Research*, vol. 15, no. 1, pp. 19782–19787, Feb. 2025, https://doi.org/10.48084/etasr.9516.

[9] M. Bilal, R. Saleem, Hammad. H. Abbasi, M. F. Shafique, and A. K. Brown, "An FSS-Based Nonplanar Quad-Element UWB-MIMO Antenna System," *IEEE Antennas and Wireless Propagation Letters*, vol. 16, pp. 987–990, 2017, https://doi.org/10.1109/LAWP.2016.2615884.

[10] M. S. Khan, A. Iftikhar, R. M. Shubair, A.-D. Capobianco, B. D. Braaten, and D. E. Anagnostou, "Eight-Element Compact UWB-MIMO/Diversity Antenna With WLAN Band Rejection for 3G/4G/5G Communications," *IEEE Open Journal of Antennas and Propagation*, vol. 1, pp. 196–206, 2020, https://doi.org/10.1109/OJAP.2020.2991522.

[11] M. M. Hasan *et al.*, "Gain and isolation enhancement of a wideband MIMO antenna using metasurface for 5G sub-6 GHz communication systems," *Scientific Reports*, vol. 12, no. 1, June 2022, Art. no. 9433, https://doi.org/10.1038/s41598-022-13522-5.

[12] J. Ren, W. Hu, Y. Yin, and R. Fan, "Compact Printed MIMO Antenna for UWB Applications," *IEEE Antennas and Wireless Propagation Letters*, vol. 13, pp. 1517–1520, 2014, https://doi.org/10.1109/LAWP.2014.2343454.

[13] N. Hussain, M.-J. Jeong, A. Abbas, T.-J. Kim, and N. Kim, "A Metasurface-Based Low-Profile Wideband Circularly Polarized Patch Antenna for 5G Millimeter-Wave Systems," *IEEE Access*, vol. 8, pp. 22127–22135, 2020, https://doi.org/10.1109/ACCESS.2020.2969964.

[14] N. C. Naik, N. K. Sahu, B. K. Ekka, and T. K. Patra, "Performance Improvement of Antenna Using Metasurface: An Overview," *Progress In Electromagnetics Research B*, vol. 101, pp. 63–84, July 2023, https://doi.org/10.2528/PIERB23050503.

[15] D. Samantaray and S. Bhattacharyya, "A Gain-Enhanced Slotted Patch Antenna Using Metasurface as Superstrate Configuration," *IEEE Transactions on Antennas and Propagation*, vol. 68, no. 9, pp. 6548–6556, Sept. 2020, https://doi.org/10.1109/TAP.2020.2990280.

[16] K. E. Kedze, H. Wang, and I. Park, "A Metasurface-Based Wide-Bandwidth and High-Gain Circularly Polarized Patch Antenna," *IEEE Transactions on Antennas and Propagation*, vol. 70, no. 1, pp. 732–737, Jan. 2022, https://doi.org/10.1109/TAP.2021.3098574.

[17] S. Tariq, S. I. Naqvi, N. Hussain, and Y. Amin, "A Metasurface-Based MIMO Antenna for 5G Millimeter-Wave Applications," *IEEE Access*, vol. 9, pp. 51805–51817, 2021, https://doi.org/10.1109/ACCESS.2021.3069185.

[18] D. A. Sehrai *et al.*, "Metasurface-Based Wideband MIMO Antenna for 5G Millimeter-Wave Systems," *IEEE Access*, vol. 9, pp. 125348–125357, 2021, https://doi.org/10.1109/ACCESS.2021.3110905.

[19] M. A. Abbas, A. Allam, A. Gaafar, H. M. Elhennawy, and M. F. A. Sree, "Compact UWB MIMO Antenna for 5G Millimeter-Wave Applications," *Sensors*, vol. 23, no. 5, Mar. 2023, Art. no. 2702, https://doi.org/10.3390/s23052702.

[20] S. Sengar, P. K. Malik, S. Das, T. Islam, R. Singh, and S. Asha, "A Quad Port MIMO Antenna Designed with an X-Shaped Decoupling Structure for Wideband Millimeter-Wave (mm-Wave) 5G FR2 New Radio (N258/N261) Bands Applications," *Wireless Personal Communications*, vol. 134, no. 2, pp. 857–880, Jan. 2024, https://doi.org/10.1007/s11277-024-10934-6.

[21] T. Raj, R. Mishra, P. Kumar, A. Kapoor, and P. Kuchhal, "Design and development of a FSS backed high gain UWB MIMO planar antenna for FR-II NR bands," *Results in Engineering*, vol. 26, June 2025, Art. no. 105034, https://doi.org/10.1016/j.rineng.2025.105034.

[22] R. Shetty, A. Singh, A. K. Bhat, S. Rao, and H. Bhat, "Miniaturized Hexagonal Antenna with Defected Ground Plane for 5G MM Wave Applications," *Progress In Electromagnetics Research C*, vol. 137, pp. 93–109, Aug. 2023, https://doi.org/10.2528/PIERC23052902.

[23] Q. Yuan *et al.*, "Recent advanced applications of metasurfaces in multi-dimensions," *Nanophotonics*, vol. 12, no. 13, pp. 2295–2315, June 2023, https://doi.org/10.1515/nanoph-2022-0803.

[24] A. Alvarez-Fernandez *et al.*, "Block Copolymer Directed Metamaterials and Metasurfaces for Novel Optical Devices," *Advanced Optical Materials*, vol. 9, no. 16, Aug. 2021, Art. no. 2100175, https://doi.org/10.1002/adom.202100175.